Determination of the acoustic damping characteristics of an annular tail-pipe.

R. Boonen [1]**, P. Sas** [2]**, E. Vandenbulck**[3]
[1] K.U.Leuven, Department of Mechanical Engineering, P.M.A.
Celestijnenlaan 300 B, B-3001, Heverlee, Belgium
e-mail: **rene.boonen@mech.kuleuven.be**

[2] K.U.Leuven, Department of Mechanical Engineering, P.M.A.
Celestijnenlaan 300 B, B-3001, Heverlee, Belgium
[3] K.U.Leuven, Department of Mechanical Engineering, T.M.E.
Celestijnenlaan 300 B, B-3001, Heverlee, Belgium

Abstract

A damping device, consisting of an annular tail-pipe, has been developed. It is applicable in situations wherein acoustic damping is required in combination with low flow resistance. Examples are ventilation systems, turbo- engines, intake and exhaust systems for internal combustion engines. The device consists of a central tube surrounded by a narrow slit. The central tube has an acoustic mass which impedance increases with frequency. When the frequency has been increased sufficiently, a considerable part of the acoustic flow passes through the slit where it will be damped. In this way, acoustic energy can be dissipated while the flow experiances a low flow resistance. The acoustic properties of the device will be investigated using an electrical equivalent model. The impedance will be measured using an impedance measurement duct. The slit resistance will be identified and the damping mechanism will be investigate qualitatively. As result, the slit resistance consists of a linear part, which depends on the air viscosity, and a non-linear part, wherein the loss of kinetic energy of the moving fluidum through the slit causes acoustic damping.

1 Introduction

Several applications require high acoustic damping in combination with low flow resistance. These applications concern for example gas flow machines such as ventilation systems, turbo-engines, intake and exhaust systems for internal combustion engines. In several cases, absorption is realised by placing resistive materials in the flow, such as fiber materials, foams, perforated plates and metal weavings. They are quite efficient to suppress noise, however they can generate a considerable pressure drop.

In this paper, a damping device will be presented, consisting of a central tube with neglectable flow resistance surrounded by a narrow slit to generate the acoustic damping. The central tube behaves as an acoustic mass which impedance is proportional to frequency. When the frequency has been increased sufficiently, a considerable part of the acoustic flow passes through the slit where it will be damped. In this way, acoustic energy can be dissipated while the flow experiances a low flow resistance. A measurement setup has been developed. The impedance of the damping device will be measured using the two microphone transfer function method according to ISO 10534-2 on an improved measurement wave guide [1]. An electrical equivalent model has been used to validate the measurement results and to extract the resistance of the slit from the measurements. The relation of the slit resistance in terms of frequency and acoustic excitation level has been investigated. A preliminairy non-linear analysis has been performed, which have to be further investigated in future research.

2 Configuration of the damping device

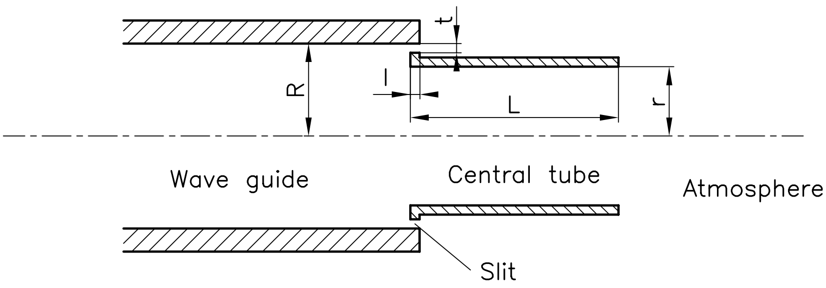

Figure 1: Scheme of the damping device.

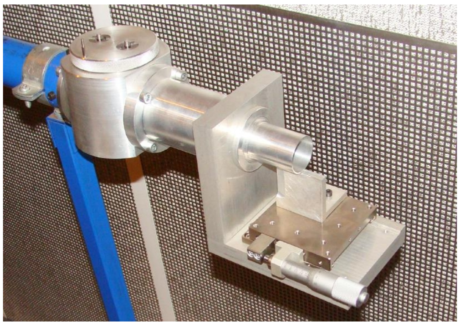

Figure 2: Photo of the damping device.

The construction of the damping device is presented in figure 1. A photograph of the device is presented in figure 2. At the left side situates the wave guide through which the waves are incoming. The wave guide consist of a duct with radius $R = 20$ mm. The damping device consists of a central tube with length $L = 45$ mm and radius $r = 15$ mm. Between the central tube and the wave guide wall, the narrow slit is situated. The slit has a length $l = 1.5$ mm and is $t = 0.1$ mm wide. Both the central tube and the slit are connected to the atmosphere at the right side.

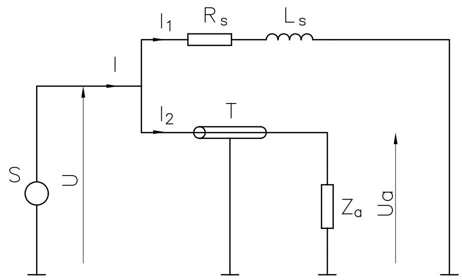

Figure 3: Electrical equivalent circuit of the damping device.

The analysis of the damping device is carried out using an equivalent electrical circuit, which is presented in figure 3. The voltage U represents the pressure p at the left side of the central tube in figure 1. The current I represents the acoustic flow Φ which divides in a current I_1 through the slit and I_2 through the central tube. The slit is represented by its resistance R_s and its acoustic mass L_s. The central tube is represented by the wave guide T with characteristic impedance $Z_c = \frac{\rho\, c}{\pi\, r^2}$ and is closed by the spherical radiator Z_a, representing the atmosphere.

In order to determine the acoustic dissipation in the slit, the currents in the two branches in the circuit have to be calculated. Therefore, the impedance of each branch will be determined. The impedance of the branch containing the central tube is determined from the transfer matrices:

$$\begin{bmatrix} U \\ I_2 \end{bmatrix} = \begin{bmatrix} \cos k\,L & j\,Z_c\,\sin k\,L \\ \dfrac{j}{Z_c}\,\sin k\,L & \cos k\,L \end{bmatrix} \begin{bmatrix} 1 & 0 \\ \dfrac{1}{Z_a} & 1 \end{bmatrix} \begin{bmatrix} U_a \\ 0 \end{bmatrix} \tag{1}$$

wherein k is the wave number, $j = \sqrt{-1}$, L the length of the central tube, Z_c the characteristic impedance of the central tube and $Z_a = \frac{\rho\,c}{\pi\,r^2}\,\frac{j\,k\,r}{1+j\,k\,r}$ the spherical radiator impedance representing the atmosphere. ρ is the air density, c the speed of sound and r the central tube radius. The impedance of the central tube Z_2 results then from equation (1):

$$Z_2 = \frac{U}{I_2} = \frac{\cos k\,L + j\,\dfrac{Z_c}{Z_a}\,\sin k\,L}{\dfrac{j}{Z_c}\,\sin k\,L + \dfrac{1}{Z_a}\,\cos k\,L} \tag{2}$$

The impedance Z_1 of the upper branch containing the slit will be:

$$Z_1 = R_s + j\,\omega\,L_s \tag{3}$$

with $\omega = 2\,\pi\,f = \frac{k}{c}$ the angle frequency, R_s the slit resistance and $L_s = \frac{\rho\,l}{2\,\pi\,R\,t}$ the acoustical mass of the slit, with $2\,\pi\,R$ the slit circumference and t the slit width. The total impedance of the device will be

$$Z = \frac{Z_1\,Z_2}{Z_1 + Z_2} \tag{4}$$

which will be measured using the two microphone transfer function method from which the slit resistance R_s will be determined.

3 Impedance and particle velocity measurement method

The impedance of the device will be measured using the two microphone transfer function method according to the standard ISO 10534-2 [2]. A scheme of the setup is presented in figure 4. It consists of a measurement

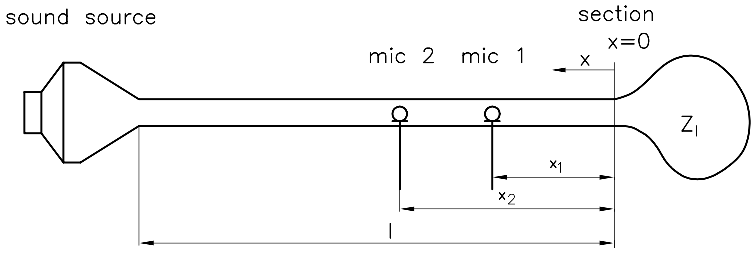

Figure 4: Scheme of the setup to measure the acoustic impedance of Z_l.

wave guide with characteristic impedance $Z_0 = \frac{\rho\,c}{\pi\,R^2}$ with at the left side an excitation loudspeaker and at the right side the impedance to be measured Z_l. This impedance includes everything present at the right side of the reference section. At two distinct positions x_1 and x_2 in the duct wall, two microphones ”mic 1” and ”mic 2” are located. First, the transfer function T_{12} between the two microphones will be measured. Then, the microphones will be exchanged in position, i.e. ”mic 1” will be positioned at location x_2 and ”mic 2” at location x_1. The transfer function T_{21} between the two microphones will be measured. The deviation in microphone characteristics will be compensated by multiplying T_{12} by the geometric mean δ of the two transfer functions:

$$\delta = \sqrt{T_{12}\, T_{21}} \tag{5}$$

The corrected transfer function $TF = \delta\, T_{12}$ is then used to calculate the unknown impedance Z_l:

$$Z_l = j\; Z_0\, \frac{\sin k\, x_1 - TF\; \sin k\, x_2}{\cos k\, x_1 - TF\; \cos k\, x_2} \tag{6}$$

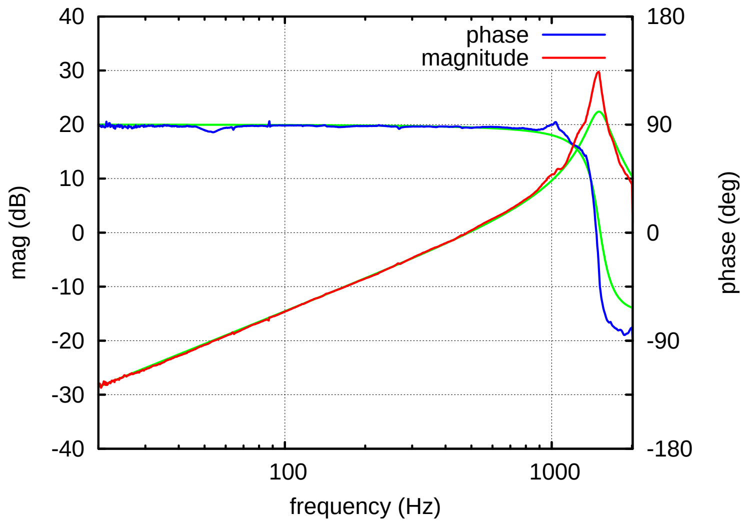

Figure 5: Comparison of the measured impedance of the device with closed slit in magnitude (red line),(reference 0dB= Z_0) and phase (blue line) and the simulated impedance with closed slit (green line).

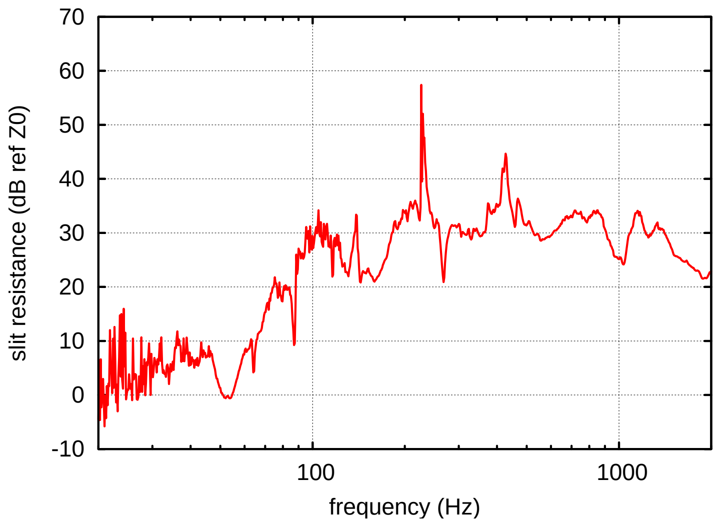

Figure 6: Measured resistance magnitude of the closed slit (reference 0dB=Z_0).

The particle velocity u at the reference section will be calculated from the linear spectra measured at the two microphone locations. In the centre between the two microphones, Eulers law is valid:

$$\frac{\mathrm{d}\,p}{\mathrm{d}\,x} = -\rho\,\frac{\mathrm{d}\,u_c}{\mathrm{d}\,t} \tag{7}$$

which can be approximated using:

$$\frac{\Delta p}{\Delta x} = -\rho\;j\;\omega\;u_c \tag{8}$$

wherein Δp is the pressure difference between the microphones and Δx the distance between the microphones and u_c the particle velocity. This expression is valid until a half wave length stands between the microphones. At 1 kHz, the deviation between expression (8) and (7) is smaller than 2%, at 2 kHz 5%. The particle velocity $u = \frac{\Phi}{\pi\,R^2}$ at the reference section will then be determined from the particle velocity u_c in the centre between the two microphones:

$$u = u_c\,\frac{1-\Gamma}{\mathrm{e}^{j\,\omega\,(x_1+x_2)/(2\,c)} - \Gamma\,\mathrm{e}^{-j\,\omega\,(x_1+x_2)/(2\,c)}}; \tag{9}$$

in which Γ is the reflection coefficient to the damping device, determined from its impedance Z and the characteristic impedance of the measurement duct Z_0:

$$\Gamma = \frac{Z - Z_0}{Z + Z_0} \tag{10}$$

4 Measurement results

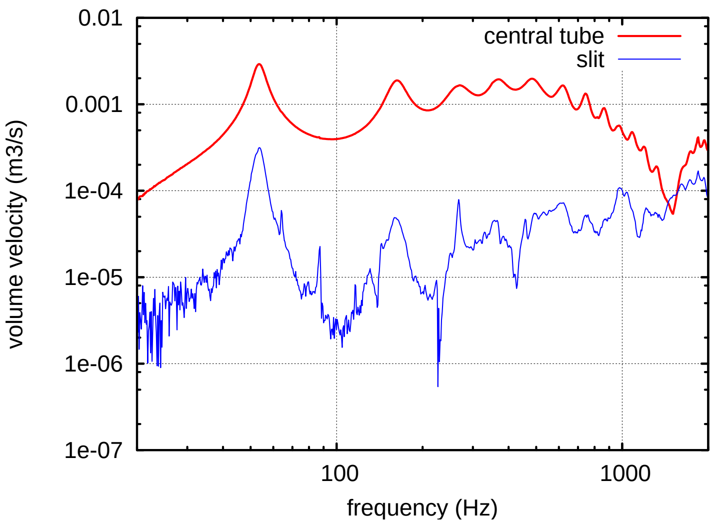

Figure 7: Volume velocity through the device (thin blue line) and through the slit (thick red line).

The measurements are carried out on the impedance duct using a dynamic signal analyser SRS785 with two PCB106B microphones. A 60W loadspeaker is excited using different voltages i.e. 10V, 20V, 30V, 60V and 100V to vary the particle velocity at the device. For each voltage, the transfer functions between the two microphones and the linear pressure spectra at each microphone have been measured. From these, the impedance Z is determined using expression (6) and the particle velocity u from expression (9). Then, from expression (4), the resistance R_s of the slit will be determined and its dependance in terms of frequency and particle velocity will be investigated.

The first set of measurements is carried out with the slit closed at its back. The impedance will be only the central tube and the volume of the slit. In figure 5, the acoustic impedance of the device at the reference section is presented in magnitude (red line) and phase (blue line). The 0 dB level corresponds to the characteristic impedance of the duct Z_0. The impedance of the central tube simulated using expression 2 is plotted over the measurement (green line). Except for the damping of the resonance of the central duct, the agreement is very well. This means that the slit properties can be reliably extracted from the impedance measurement until about 1 kHz.

The magnitude of the slit resistance, determined from the impedance measurement presented in figure 5 using expressions (4) and (3), is plotted in figure 6. This result can be interpreted as the maximum measurable resistance, as theoretically it should be infinite. Above 100 Hz, the measurable resistance rises above 20 dB ($10 \times Z_0$) until 30 dB ($30 \times Z_0$).

Figure 7 presents the volume velocity determined using expression (9) through the damping device (thick red line) and through the slit (thin blue line) when applying 60 V on the loudspeaker. The slit volume velocity is about 1% of the total velocity.

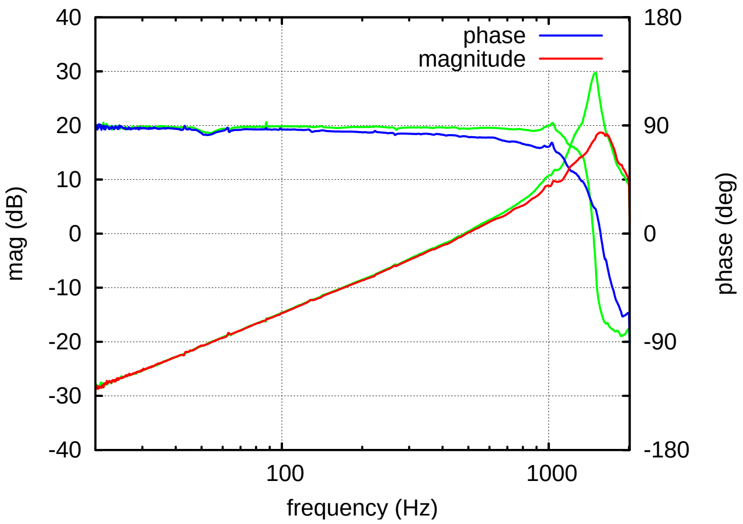

Figure 8: Comparison of the impedance of the device with open slit in magnitude (red line),(reference 0dB= Z_0) and phase (blue line) and the impedance with closed slit (green line).

The second set of measurements is carried out with open slit. The same methods are applied as in the first set. Figure 8 presents the measured device impedance in magnitude (red line) and phase (blue line) when 60 V has been applied on the loudspeaker. The measured impedance of the closed slit has been plotted over it (green line). The difference between the two graphs demonstrates a considerable effect of the slit on the total impedance. The particle velocity through the slit, presented in figure 9, has been measured with increasing loadspeaker level, i.e. the lowest curve is measured using 10 V, the curve above with 20 V, then 30 V, 60 V until the upper curve with 100 V.

The slit resistance, obtained from the measured impedance, is presented in figure 10 in magnitude (reference 0 dB= Z_0) and in figure 11 in phase for all applied voltages to the loudspeaker. The resistance magnitude increases with the loadspeaker level, i.e. the lowest curve is measured using 10 V, the curve above with 20 V, then 30 V, 60 V until the upper curve with 100 V. The measured resistance is below the level displayed in figure 6 and will be reliable starting from 100 Hz. The phase of the slit resistance, presented in figure 11, lies for all loudspeaker levels around the zero degrees, which confirms the resistive nature of the slit. The curves do not follow the sequence of the loudspeaker levels such as the resistance magnitudes do. The real part of the slit resistance (thick red lines) in terms of the particle velocity through the slit is presented in figure 12 for different frequencies. Each curve consists of five points and exhibits a linear relationship between the

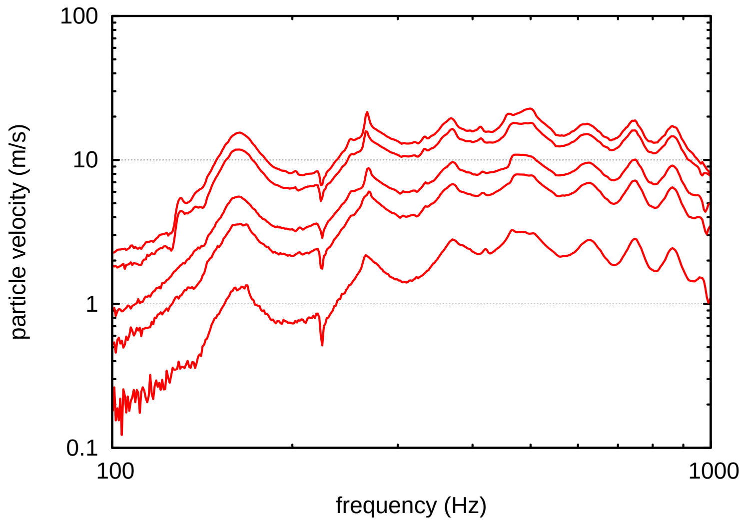

Figure 9: Particle velocity through the slit in terms of frequency for different loudspeaker excitation levels. Lowest curve: 10V, curve above 20V and so on for 30V, 60V to the upper curve 100V.

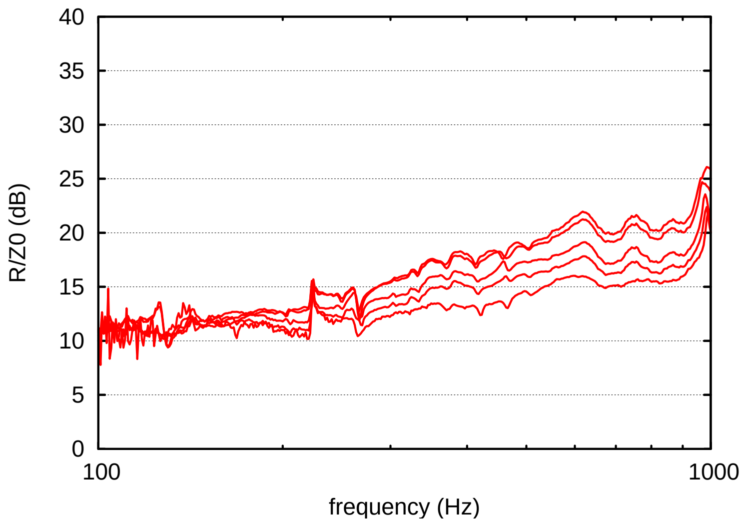

Figure 10: Magnitude of the slit resistance in terms of frequency for different loudspeaker excitation levels. Lowest curve: 10V, curve above 20V and so on for 30V, 60V to the upper curve 100V.

slit resistance and the particle velocity through it. There is no definite sequence of the curves in terms of frequency, which suggests that there is no relation between the slit resistance and frequency. The imaginairy part of the slit resistance, from which the acoustic mass has been eliminated, is presented in figure 13. The reactance magnitude is considerably smaller than the real part and tends to be constant in terms of particle velocity. The reactance tends to increase with frequency.

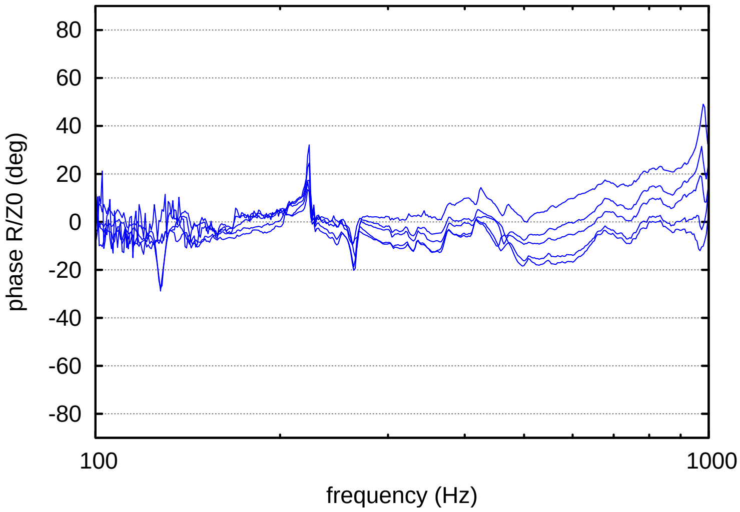

Figure 11: Phase of the slit resistance in terms of frequency for different loudspeaker excitation levels.

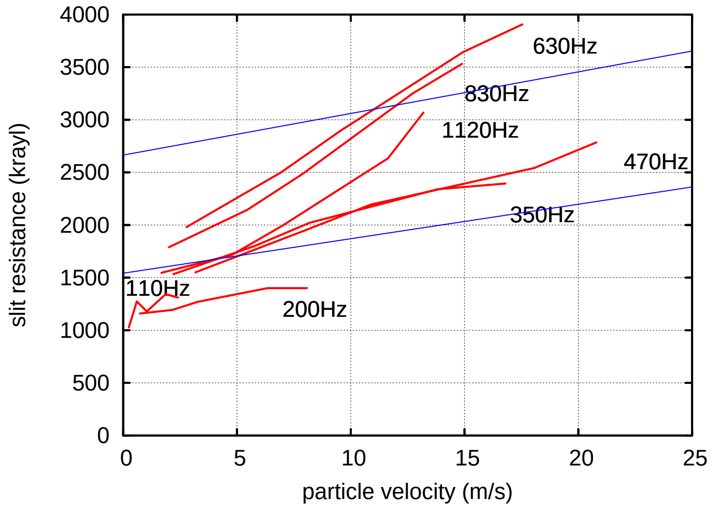

Figure 12: Slit resistance in terms of particle velocity through the slit for different frequencies (thick red lines: measured, thin blue lines: simulated using expression (18)).

5 Qualitative analysis of the slit resistance

The slit resistance can be considered as the sum of a linear part (constant resistance) and a non-linear part, which depends on the particle velocity through the slit. The linear resistance R_{sa} can be obtained using [3]:

$$R_{sa} = \frac{12\,\eta\,l}{2\,\pi\,R\,t^3} \tag{11}$$

wherein $\eta = 18.6 \cdot 10^{-6}$ Ns/m^2 the vicosity of air, l the slit length, $2\,\pi\,R$ the slit circumference and t the slit width.

To obtain the velocity dependent part, the loss of kinetic energy of the flow will be considered [4, 5]. Figure 14 shows the situation. Before entering the slit, the mass $\rho\,S\,u_s\,\mathrm{d}\,t$ has a velocity u_0 and flows through an area S_0 which is larger than the slit cross-section S. When this mass has to flow through the slit, is has to

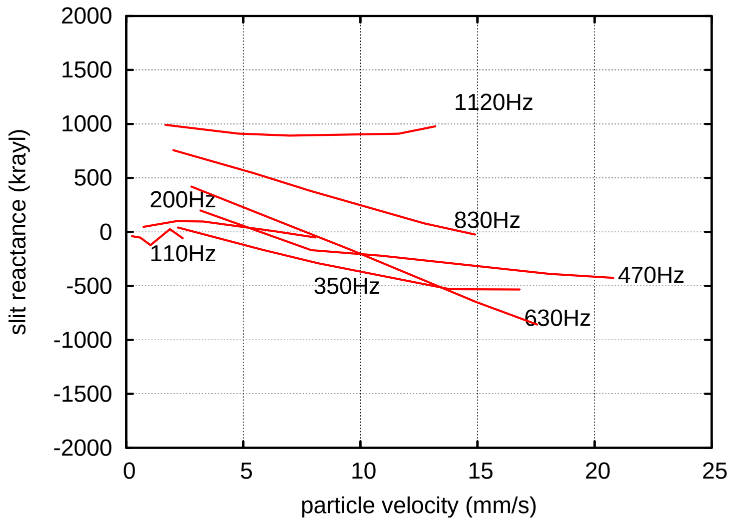

Figure 13: Measured slit reactance in terms of particle velocity through the slit for different frequencies.

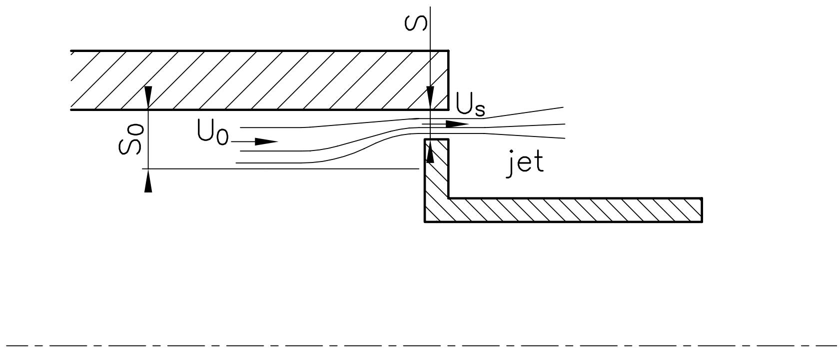

Figure 14: Contraction of the flow through the slit.

contract from the surface S_0 to $S = 2\,\pi\,R\,t$ of the slit and the mass accelerates until it reaches the velocity u_s. This is demonstrated in figure 15, where the slit velocity (thick red line) increases until 10 times the incoming particle velocity u_0 (thin blue line) due to the surface contraction from S_0 to S. When this mass exits the slit at the other side, a jet will be formed due to the sudden area jump and the kinetic energy of the mass will be dissipated. When the flow alternates, this process happens at both sides of the slit. Altouch the geometric situation is different at both sides of the slit, it is assumed that the process is the same at both sides. For alternating flow, the difference in kinetic energy W of the mass $\rho\,S\,u_s\,\mathrm{d}\,t$ moving through the slit compared to before entering the slit, expressed for a half period T, will be:

$$W = \int_0^{T/2} \rho\,S\,u_s\,\frac{u_s^2 - u_0^2}{2}\,\mathrm{d}\,t \tag{12}$$

The volume velocity before the slit and in the slit will be equal, so $\Phi = u_0\,S_0 = u_s\,S$. The surface ratio between the cross-section which the flow passes through before the slit and the cross-section of the slit itself is $\sigma = \frac{S}{S_0} = \frac{u_0}{u_s}$. Expressing the work W in terms of the particle velocity through the slit u_s gives:

$$W = \int_0^{T/2} \frac{1}{2}\,\rho\,S\,(1-\sigma^2)\,u_s^3\,\mathrm{d}\,t \tag{13}$$

In case of harmonic excitation, i.e. $u_0 = u\,\sin\omega t$, the velocity through the slit will be $u_s = \frac{u\,\sin\omega t}{\sigma}$. The

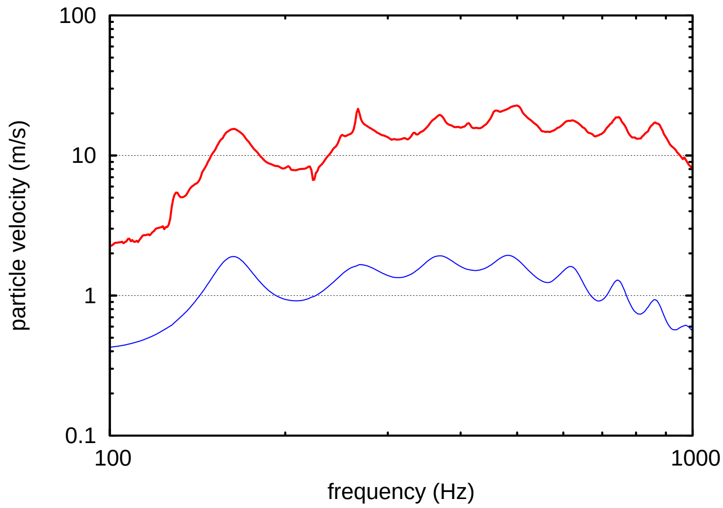

Figure 15: Particle velocity u_0 before the slit (thin blue line) and u_s through the slit (thick red line) while contracting from the surface S_0 to S with a loudspeaker excitation level of 100V.

integral will be evaluated for a half period of the sine wave, resulting in:

$$W = \frac{2}{3\,\omega}\rho\, S\,\frac{1-\sigma^2}{\sigma^3}\,u^3 \tag{14}$$

In analogy to electrical engineering, the resistance R_{su} will be determined from the dissipation energy:

$$W = \int_0^{T/2} R_{su}\,\Phi^2\,\mathrm{d}\,t = \int_0^{T/2} R_{su}\,S^2\,u_s^2\,\mathrm{d}\,t \tag{15}$$

Replacing u_s by $\frac{u\,\sin\omega t}{\sigma}$ and evaluating the integral results in:

$$W = R_{su}\,\frac{\pi}{2\,\omega}\,S^2\,\frac{u^2}{\sigma^2} \tag{16}$$

The non-linear part of the slit resistance R_{su} will result by equating expression (16) with (14):

$$R_{su} = \frac{4}{3\,\pi}\,\frac{\rho}{S}\,\frac{1-\sigma^2}{\sigma}\,u \tag{17}$$

The resulting resistance R_{su} is independent of frequency and proportional to the particle velocity u, which appears also from the measured resistance presented in figure 12. When $\sigma = 1$, which means that there is no (sudden) area change before and through the slit, the slit will exhibit no flow induced damping. Sudden area jumps are crucial for flow induced damping.

The total resistance of the slit is the sum of the linear and the non-linear part:

$$R_s = \frac{12\,\eta\,l}{2\,\pi\,R\,t^3} + \frac{4}{3\,\pi}\,\frac{\rho}{S}\,\frac{1-\sigma^2}{\sigma}\,u \tag{18}$$

The numerical values for the geometry and viscosity are putted in equation (18). The cross-section ratio $\sigma = 0.1$ is deduced from the particle velocities from figure 15. The result is plotted in figure 12 (thin blue line). The lower line is simulated for a slit of $.12$ mm width and the upper line for $.10$ mm width. The viscous part of the slit resistance is very sensitive to small variations of the slit width. The slope of the resistance, which is the flow induced part, is about a factor 1.5 too small compared to the measurements. For the rest, the values of the calculated resistance are in the right order of magnitude as the measured resistance, which indicates that the assumption of the forming of jets is the correct damping mechanism for the non-linear part of the slit resistance. This will be subject to further future research.

6 Conclusion

A damping device, consisting of a central tube surrounded by a narrow slit, has been investigated. It has a neglectable flow resistance. The impedance of the acoustic mass of the central tube increases with frequency. At higher frequencies, a considerable part of the acoustic flow passes through the slit, where it will be damped. The damping mechanism is two fold: a linear part of the slit resistance in which the viscosity of the air is involved and a non-linear part wherein the slit resistance is proportional to the particle velocity of the air through the slit. In this part, the loss of kinetic energy of the pulsing flow due the abrupt cross-section jumps before and after the slit causes additional flow induced damping. Further research will be carried out to investigate the formation of the jet behind the slit. Ultimately, this research will result in development rules for such devices and to optimize the geometry of the annular tube for specific applications.

Acknowledgements

The author thanks the F.W.O. (Fonds Wetenschappelijk Onderzoek) for funding this research project.

References

[1] R. Boonen, P. Sas, W. Desmet, W. Lauriks, G.Vermeir, *Calibration of the two microphone transfer function method with hard wall impedance measurements at different reference sections* , Journal of the Mechanical Systems and Signal Processing, Vol. 23, No. 5, (2009), pp. 1662-1671.

[2] ISO 10534, *Determination of sound absorption coefficient and impedance in impedance tubes* , International Organisation for Standardization, Case postale 56, CH-1211 Genève 20, (1998).

[3] L. L. Beranek, *Acoustics* , Mc Graw-Hill, (1954)

[4] L. J. Sivian, *Acoustic impedance of small orifices*, Journal of the Acoustical Society of America, Vol. 7, (1935), pp. 94-101.

[5] U. Ingard, S. Labate, *Acoustic circulation effects and the nonlinear impedance of orifices*, Journal of the Acoustical Society of America, Vol. 22, No. 2, (1949), pp. 211-218